

## CHAPTER - IX

### SUMMARY AND CONCLUSIONS

Thin film science has wide sprayed applications in many fields of science and technology which is consisted of materials science, surface science and applied physics. The range of thin film applications is so vast that it extends from micrometer dots in microelectronics to coatings of several square meters on window glasses. The rapid progress in thin film micro and nano materials has given birth to a whole new technology of junction devices and integrated circuits of monoliths and hybrid types.

The search for new thin film materials appropriate to solar cell applications is of particular importance. Features such as the electronic structure, mobilities and the characteristic optical absorption are frequently those that determine material stability. The properties of thin film materials are ultimately connected with the method of their fabrication. Hence, the search for new materials also implies the exploration of fabrication process. Cheapness is also one of the important criterion for solar cell fabrication. The development of thin film technology for the fabrication of large area photodiode arrays using physical and chemical deposition techniques has turned chemical kinetics into one of the most active field of the electrochemistry.

Electrochemical photovoltaic (ECPV) cells for the conversion of solar energy into either electrical or chemical energy is one of the attractive, efficient and reliable tools; which seems to be a promising answer to the problem of

energy crises in the decade. Much attention is given to the formation and improvement of ECPV cells and new materials for solar energy conversion are searched out. In order to reduce the cost and have the quick access to the physico–chemical properties of the materials, a relatively simple and quick deposition process is preferred.

Antimony Sulphide and Antimony Selenide are the layer structured photoactive semiconductors, which have received a little attention as a prospective material in ECPV cells. Considering the importance and scope of the subject in the present investigation, the studies are made on preparation and physico–chemical characterization of antimony chalcogenide thin films prepared from aqueous and non– aqueous media by the spray pyrolysis technique. Their (photo)electrochemical characteristics and use in rechargeable separator–storage cells has been investigated. The present work is divided into nine phases.

The **first chapter** is introductory in nature. A brief survey of literature on  $Sb_2S_3$  and  $Sb_2Se_3$  material is given which is followed by the scope of the present work.

The theoretical background of various characterization techniques such as X-ray diffraction, scanning electron microscopy (SEM), optical absorption, transport properties viz. Electrical resistivity, thermoelectric power etc. is outlined in **chapter–II**. The theory of semiconductor – electrolyte interface, Helmholtz and Gouy–Chapman layer, Stern model along with conversion of

light energy into electricity via photoelectrochemical route have been discussed in this chapter. The concept of using semiconductor– septum (SC–SEP) as an energy storage system, storage in the form of electrical energy and hydrogen using SC–SEP have also been discussed in it.

**Chapter – III** opens with the introduction of one of the simplest thin film deposition technique “spray pyrolysis”. It mainly deals with the spray deposition and physicochemical characterization of  $\text{Sb}_2\text{S}_3$  thin films from aqueous medium.  $\text{Sb}_2\text{S}_3$  thin films were deposited by spraying an aqueous tartaric acid complex of  $\text{SbCl}_3$  and  $\text{CH}_3\text{CSNH}_2$  onto preheated amorphous glass substrates. The films were prepared by taking equimolar solutions of  $\text{SbCl}_3$  and  $\text{CH}_3\text{CHNS}_2$  in appropriate volumes so as to obtain Sb: S ratio of 2:3. The spray rate was kept constant at  $5 \text{ cc min}^{-1}$ . 3 cc solution of tartaric acid was mixed with 6 cc of  $\text{SbCl}_3$ . Then 9 cc of  $\text{CH}_3\text{CSNH}_2$  solution was added into complexed  $\text{SbCl}_3$  and immediately sprayed onto hot glass substrates maintained at  $300 \text{ }^\circ\text{C}$ . When the sprayed droplets of the mixed solution reach to the hot substrate, pyrolytic decomposition occurs and desired  $\text{Sb}_2\text{S}_3$  film is formed on the substrates. The effect of preparative parameters such as spray rate, substrate temperature concentration of tartaric acid and concentration of spraying solution on the film quality; in terms of crystallinity, resistivity etc. has been studied. Following are the optimized preparative parameters for  $\text{Sb}_2\text{S}_3$  thin films from aqueous media.

1.	Solutions used	0.075M $\text{SbCl}_3$ (aq.) + 0.5 M tartaric acid (aq.) + 0.075 M $\text{CH}_3\text{CSNH}_2$ (aq.)
2.	Substrates	Glass microslides and FTO coated glass substrates
3.	Substrate Temperature	300 °C
4.	Spray rate	5 cc min <sup>-1</sup>
5.	Quantity of solution sprayed	18 cc
6.	Film thickness	0.5 μm

The structural, optical and electrical characterization of the films deposited at optimized preparative parameters is carried out by means of X-ray diffraction (XRD) scanning electron microscopy (SEM) optical absorption, dark electrical resistivity and thermoelectric power measurement techniques.

The XRD patterns of the films are recorded in the range of diffracting angle 10° to 100°. The appearance of the broad X-ray spectrum suggests that the films are either amorphous or of poor crystallinity (microcrystalline).

SEM micrographs of  $\text{Sb}_2\text{S}_3$  thin films deposited onto the glass substrates show the irregular particle growth with uneven surface morphology. The total substrate surface is covered by the film with rough surface with random distribution of overgrown particles.

The optical characterization of  $\text{Sb}_2\text{S}_3$  thin films is carried out by

measuring the optical density ( $\alpha t$ ) in the wavelength range of 350 to 850 nm. The films show cut-off at 690 nm. The optical gap of spray deposited  $\text{Sb}_2\text{S}_3$  is found to be 1.8 eV.

The dark electrical resistivity measurements are carried out with two point d.c. probe method. These measurements show that the prepared  $\text{Sb}_2\text{S}_3$  films have high resistivity and is of the order of  $10^6 - 10^7 \Omega\cdot\text{cm}$ . From the  $\log \rho$  versus  $1/T$  plot it is found that resistivity decreases with increase in temperature and suggests the semiconducting behavior of  $\text{Sb}_2\text{S}_3$  films. The estimated activation energy is equal to 0.52 eV.

The thermoelectric power measurements were used to determine the conductivity type exhibited by  $\text{Sb}_2\text{S}_3$  films. The thermoelectric voltage to the temperature difference across the piece of the semiconductor, which is also known as seebeck coefficient. The temperature difference causes a transport of carriers from hot to cold end and thus creates the electric field which gives rise to thermal voltage. It is seen that the polarity of thermoelectric voltage for  $\text{Sb}_2\text{S}_3$  films is positive towards the hot end, indicating the  $\text{Sb}_2\text{S}_3$  is *n*-type in nature. The plot of TEP versus temperature shows that TEP increases with increase in temperature, which can be attributed to the increase in carrier concentration and mobility of the charge carriers with rise in temperature.

In **Chapter–IV** emphasis is given on preparation and characterization of  $\text{Sb}_2\text{S}_3$  thin films from non-aqueous medium. The solutions of  $\text{SbCl}_3$  and  $\text{CS}(\text{NH}_2)_2$  are prepared by dissolving required amounts of the salts in acetic

acid (glacial) and their equimolar quantities are mixed together in appropriate volumes to obtain Sb: S ratio of 2:3. The mixed solution is kept about 12 hours so that the yellowish turbidity disappears and clear solution is obtained. The effect of preparative parameters such as spray rate, substrate temperature and concentration of spraying on the crystallinity of the films has been discussed. The optimized deposition parameters are as follows:

- |                                 |                                                                                                                  |
|---------------------------------|------------------------------------------------------------------------------------------------------------------|
| 1. Solutions used               | 0.1M $\text{SbCl}_3$ in acetic acid + 0.1 M $\text{CS}(\text{NH}_2)_2$ in acetic acid in volumetric ratio of 2:3 |
| 2. Nature of the substrates     | Glass microslide and FTO coated glass                                                                            |
| 3. Substrate temperature        | 250 °C                                                                                                           |
| 4. Spray rate                   | 10 cc min <sup>-1</sup> .                                                                                        |
| 5. Quantity of solution sprayed | 30 cc.                                                                                                           |
| 6. Film thickness               | 0.5 μm                                                                                                           |

The  $\text{Sb}_2\text{S}_3$  compound formation is analyzed with the help of XRD patterns and it shows a single well-defined peak in the direction of plane (060). The orientations along (310), (111), (211), (221) and (301) have also been observed with relatively smaller XRD peak intensity. Thus the material formed is polycrystalline in nature. The calculated lattice parameters for orthorhombic crystal of  $\text{Sb}_2\text{S}_3$  are found to be  $a_0 = 11.184 \text{ \AA}$  (std. 11.299 Å),  $b_0 = 11.335 \text{ \AA}$  (std. 11.31 Å) and  $c_0 = 3.835 \text{ \AA}$  (std. 3.839 Å). The grain size of  $\text{Sb}_2\text{S}_3$  films, calculated using the Scherrer's relation, is found to be 321 Å

The surface morphology of the  $\text{Sb}_2\text{S}_3$  thin film is studied by SEM micrographs, which shows the uneven surface morphology with random distribution of over grown particles. The film surface is rough and shows the presence of extra particles.

The optical absorption studies were carried out in the wavelength range of 350 to 850 nm. The variation of optical density ( $\alpha t$ ) with wavelength ( $\lambda$ ) shows that the optical absorption coefficient ' $\alpha$ ' is a function of photon energy and is found to be of the order of  $10^4 \text{ cm}^{-1}$  indicating the presence of direct band edge. The band gap energy is obtained by extrapolating the linear portion of the  $(\alpha h\nu)^2$  versus  $h\nu$  plot to the energy axis at  $\alpha = 0$  which is found to be 1.8 eV due to direct interband transition.

The two point d.c. dark resistivity measurements show that the prepared thin films have dark resistivity in the order of  $10^6 - 10^7 \Omega \cdot \text{cm}$ . The variation of  $\log(\rho)$  with reciprocal of temperature shows that the resistivity decreases with increase in temperature and supports the semiconducting nature of  $\text{Sb}_2\text{S}_3$  thin films. The activation energy is found to be 0.86 eV, which is very near to the value reported (0.9 eV) for single crystal  $\text{Sb}_2\text{S}_3$ . The results supports the formation of perfect or nearly perfect stoichiometric compound ( $\text{Sb}_2\text{S}_3$ ) using non-aqueous medium.

$\text{Sb}_2\text{S}_3$  thin films prepared from non-aqueous medium exhibit *n*-type conductivity as has been determined from TEP measurements. It is seen that TEP increases with an increase in temperature.

Annealing of  $\text{Sb}_2\text{S}_3$  thin film is carried out at  $200\text{ }^\circ\text{C}$  in nitrogen atmosphere for 2 hours to study the effect on crystallinity and grain size. The increase in grain size from 321 to  $350\text{ \AA}$  has been observed after annealing. The calculated values of lattice parameters of annealed  $\text{Sb}_2\text{S}_3$  thin films are 11.289, 11.333 and  $3.813\text{ \AA}$  respectively.

**Chapter – V** deals with the preparation and characterization of  $\text{Sb}_2\text{Se}_3$  thin films from aqueous medium using two Se sources viz.  $\text{SeO}_2$  and  $\text{CSe}(\text{NH}_2)_2$ . For both the films tartaric acid was used as complexing agent. Various optimized preparative parameters used for the deposition of  $\text{Sb}_2\text{Se}_3$  thin films from aqueous medium are listed below.

	$\text{SeO}_2$	$\text{CSe}(\text{NH}_2)_2$
1. Solutions used	0.1M $\text{SbCl}_3$ (aq.) + 0.5 M tartaric acid (aq.) + 0.1 M $\text{SeO}_2$ (aq.)	0.01M $\text{SbCl}_3$ (aq.) + 0.5M tartaric acid (aq.) + 0.01M $\text{CSe}(\text{NH}_2)_2$
2. Substrates used	Glass microslides and FTO coated glass	Glass microslides and FTO coated glass
3. Substrates temperature	$300\text{ }^\circ\text{C}$	$275\text{ }^\circ\text{C}$
4. Spray rate	$3\text{ cc min}^{-1}$	$5\text{ cc min}^{-1}$
5. Quantity of solution sprayed	30 cc	30 cc
6. Film thickness	$0.46\text{ }\mu\text{m}$	$0.51\text{ }\mu\text{m}$

The XRD patterns of the films prepared using selenium dioxide (SDO) reveals that the material formed ( $\text{Sb}_2\text{Se}_3$ ) is amorphous in nature. While the  $\text{Sb}_2\text{Se}_3$  films prepared using selenourea (SU) are polycrystalline with orthorhombic crystal structure. The calculated lattice constants are found to be  $a = 12.181 \text{ \AA}$ ,  $b = 11.290 \text{ \AA}$  and  $c = 4.038 \text{ \AA}$  which are very close to the values for single crystal  $\text{Sb}_2\text{Se}_3$ . The structural difference between the  $\text{Sb}_2\text{Se}_3$  films prepared using SDO and SU as Se source is partly owing to (i) The different substrate temperatures of the decomposition for two sources and (ii) difference in stoichiometric proportion occurred during pyrolytic decomposition of the material for two sources.

From the SEM analysis it is seen that the films prepared using SDO are continuous with fine grains. The film surface is rough and shows the presence of overgrown particles. SEM micrographs of  $\text{Sb}_2\text{Se}_3$  films prepared using SU shows total coverage of the substrate by the films with rough surface. It also shows the random distribution of a overgrown particles.

The optical absorption studies were carried out for both the films in the wavelength range 350 to 1200 nm. An Exponential increase of optical absorption coefficient at band edge have been found for the amorphous (films with SDO) films while steep absorption edge have been observed for polycrystalline (films with SU) films. The bandgap energy, obtained by extrapolating the linear portions of the  $(\alpha h\nu)^{1/2}$  versus  $h\nu$  plot for amorphous

films and  $(\alpha h\nu)^2$  versus  $h\nu$  plot for polycrystalline  $\text{Sb}_2\text{Se}_3$  films to the energy axis at  $\alpha=0$  is found to be 1.28 eV and 1.26 eV respectively. The values of the energy gap for the amorphous and polycrystalline  $\text{Sb}_2\text{Se}_3$  films are close considering that the short range orders in the two phases are identical.

Two point d. c. probe method for measuring the dark resistivity shows that both the films are semiconducting. Polycrystalline films have dark resistivity of the order of  $10^7 \Omega\cdot\text{cm}$ , whereas it is  $10^5 - 10^6 \Omega\cdot\text{cm}$ , for amorphous films. The observed activation energies, within the temperature range 350 – 450 K, are 0.63 and 0.77 eV for amorphous and polycrystalline films respectively. The difference in activation energies for these films may be attributed to the difference in density of gap states and in band tails.

TEP studies reveal that the thermo e.m.f. varies linearly with temperature difference for both the films. Thus TEP does not vary with the temperature over the temperature range studied. Positive polarity of generated thermoelectric voltage has been found, which suggests that the conduction in both the films has been of  $p$ -type. The observed values of TEP are 1.82 mV/ $^\circ\text{C}$  and 45  $\mu\text{V}/^\circ\text{C}$  for amorphous and polycrystalline films respectively.

In **Chapter – VI** emphasis is given on the preparation and characterization of  $\text{Sb}_2\text{Se}_3$  thin films from non-aqueous medium using two Se sources as SDO and SU. Solutions of  $\text{SbCl}_3$  and  $\text{SeO}_2$  were prepared by dissolving the appropriate amount of salts in acetic acid glacial and

formaldehyde, respectively. The equimolar solutions were mixed together in the appropriate volumes to obtain Sb:Se ratio as 2:3. The whitish turbidity resulted due to direct mixing of  $\text{SbCl}_3$  and  $\text{SeO}_2$  can be redissolved by the addition of excess acetic acid (glacial). Similarly, For film preparation using  $\text{CSe}(\text{NH}_2)_2$ , SU was dissolved in acetic acid (glacial) and equimolar solutions of  $\text{SbCl}_3$  and  $\text{CSe}(\text{NH}_2)_2$  were mixed together in appropriate volumes to obtain Sb:Se ratio of 2:3. Various preparative parameters used for the deposition of  $\text{Sb}_2\text{Se}_3$  thin films from non-aqueous medium are listed below.

	$\text{SeO}_2$	$\text{CSe}(\text{NH}_2)_2$
1. Solutions used	0.025M $\text{SbCl}_3$ in acetic acid(glacial) + 0.025 M $\text{SeO}_2$ in formaldehyde	0.01M $\text{SbCl}_3$ (aq.) + 0.01M $\text{CSe}(\text{NH}_2)_2$ in acetic acid (glacial)
2. Substrates used	Glass microslides and FTO coated glass	Glass microslides and FTO coated glass
3. Substrates temperature	200 $^\circ\text{C}$	150 $^\circ\text{C}$
4. Spray rate	14 cc min $^{-1}$	3 cc min $^{-1}$
5. Quantity of solution sprayed	50 cc	28 cc
6. Film thickness	1.3 $\mu\text{m}$	0.52 $\mu\text{m}$

The XRD patterns of the  $\text{Sb}_2\text{Se}_3$  films prepared using both the Se sources reveal that the material formed is amorphous

in nature.

From the SEM analysis it is seen that for the as deposited films of  $\text{Sb}_2\text{Se}_3$  there is total coverage of the substrate by the film with rough surface morphology. SEM micrographs of annealed  $\text{Sb}_2\text{Se}_3$  films exhibits its Microstructure. Random distribution of particles having different size are observed. The film is continuous with presence of extra particles. SEM micrographs of as-deposited  $\text{Sb}_2\text{Se}_3$  films prepared using  $\text{CSe}(\text{NH}_2)_2$  demonstrate an uneven surface morphology devoid of any irregular crystalline growth. Incomplete decomposition of the particles at the film surface is also seen.

The optical absorption studies were carried out for both films in the wavelength range 350 to 1200 nm. The values of the optical gaps, obtained from  $(\alpha h\nu)^{1/2}$  vs.  $h\nu$  plot for films prepared using SDO and SU is found to be 0.86 eV and 1.45 eV respectively.

Two point d.c. probe method for measuring the dark resistivity shows that both films are semiconducting and have dark resistivity of the order of  $10^6$  –  $10^7$   $\Omega\cdot\text{cm}$ . The observed activation energies are 0.77 eV and 0.82 eV for the films prepared using SDO and SU respectively.

TEP studies reveal that the conduction is both the films is of  $p$ -type. Relatively smaller thermoemf have been observed for  $\text{Sb}_2\text{Se}_3$  films prepared using  $\text{CSe}(\text{NH}_2)_2$  than prepared using  $\text{SeO}_2$ .

The  $\text{Sb}_2\text{Se}_3$  films were annealed in  $\text{N}_2$  atmosphere at an optimized

temperature of 325 °C for 2 hours in order to see the effect of annealing on physico–chemical properties of Sb<sub>2</sub>Se<sub>3</sub> films.

XRD patterns of annealed Sb<sub>2</sub>Se<sub>3</sub> films prepared using SDO reveal that the amorphous films have converted into polycrystalline after annealing. The calculated lattice constants are found to be  $a = 11.188 \text{ \AA}$ ,  $b = 11.214$  ( and  $c = 4.034$  (for orthorhombic crystal structure. Estimated bandgap energy for polycrystalline Sb<sub>2</sub>Se<sub>3</sub> from  $(\alpha h\nu)^2$  vs.  $h\nu$  plot is 2.14 eV. The change in nature and value of optical band gap after annealing the films at specific temperature may be due to (i) the change in the atomic order in the amorphous phase after annealing and occurrence of ‘wrong bonds’ due to presence of 5 fold ring in amorphous structure. After annealing, no remarkable change in the dark resistivity have been observed. From the plot of logs against  $1/T$ , it is seen that there are two regions corresponding to low and high temperatures. The activation energies corresponding to the low and high temperature regions are 0.52 eV and 1.01 eV respectively. From TEP measurement the Sb<sub>2</sub>Se<sub>3</sub> films (annealed) are found to exhibit *p*-type conductivity.

In **Chapter –VII**, the construction of PEC cell along with the experimental setup for electrical and optical characterization by PEC characterization is discussed. The requisites for photoelectrode, electrolyte and counter electrode and also discussed in this chapter. The performance parameters studied include open circuit voltage ( $V_{oc}$ ), short circuit current

( $I_{sc}$ ), junction ideality factor ( $n$ ), fill factor ( $ff$ ), efficiency ( $\eta$ ), series and shunt resistance etc. Various physical parameters of the semiconductor and semiconductor– electrolyte junction band edge locations have been reported.

Spray deposited antimony chalcogenide (namely  $Sb_2S_3$  and  $Sb_2Se_3$ ) prepared on FTO coated glass from aqueous and non–aqueous media were tested for their photoactivity by using them in photoelectrochemical (PEC) solar cell. All the films show photoactivity only in polyiodide electrolyte. Irrespective of the preparation medium,  $Sb_2S_3$  and  $Sb_2Se_3$  found to have  $n$ - and  $p$ -type conductivity respectively. Following are the results obtained on  $V_{oc}$  and  $I_{sc}$  for the films prepared on FTO coated glass substrates.

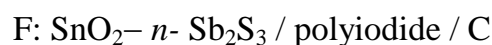
Film	$I_{sc}$ (A)	$V_{oc}$ (mV)
A – $Sb_2S_3$	1	35
NA – $Sb_2S_3$	800	209
A – $Sb_2Se_3$ (SDO)	0	2
NA – $Sb_2Se_3$ (SDO)	0.2	12
A – $Sb_2Se_3$ (SU)	1.5	10
NA – $Sb_2Se_3$ (SU)	0	6

A– Aqueous, NA – Non– Aqueous

It is found that only NA–  $Sb_2S_3$  films deposited on FTO glass titanium and stainless steel showed the acceptable performance in PEC cell. Therefore

only NA-  $\text{Sb}_2\text{S}_3$  films were further used in PEC characterization and for calculation of physical parameters of the material.

PEC solar cell was fabricated using the electrode configuration, comprising *n*-  $\text{Sb}_2\text{S}_3$  thin film as a photoanode, graphite as a counter electrode and saturated calomel Electrode (SEM) as a reference. Polyiodide was used as a electrolyte with KCl as a supporting electrolyte having composition 0.5M KCl + 0.5 M KI + 0.01 M  $\text{I}_2$ . The PEC cell has the configuration



It is observed that even in dark PEC cell gives some dark voltage with negative polarity towards  $\text{Sb}_2\text{S}_3$  electrode. The origin of this voltage is attributed to the difference between two half-cell potentials of the electrodes in the PEC cell. After illumination of the junction, cathodic behavior of photovoltage of the semiconductor is observed which indicates that the  $\text{Sb}_2\text{S}_3$  films are of *n*-type.

Current voltage (I-V) characteristic of PEC cell in dark and under illumination are studied at room temperature. The nature of the I – V curves indicate the formation of rectifying junction and the cell is a generator of electricity. The junction ideality factor was estimated from  $\log(I)$  against V plot in dark and leads to a value of 2.11.

The photoresponse of the cell is studied by noting the  $I_{sc}$  and  $V_{oc}$  of the PEC cell as a function of light intensity ( $F_L$ )  $I_{sc}$  shows linear variation with an excitation level and  $V_{oc}$  saturates at the higher values of  $F_L$ . The junction

ideality factor in light is calculated from the slope of the plot  $\log(V_{oc})$  against  $F_L$ , which comes out to be 1.34. Various parameters obtained from power output plots using  $n$ -  $Sb_2S_3$  films on various substrates under various conditions are tabulated below

Condition of film	Isc ( $\mu\text{A}/\text{cm}^2$ )	Voc (mV)	$\eta$ (%)	ff (%)	$R_s$ ( $\Omega$ )	$R_{sh}$ ( $\text{K}\Omega$ )
Titanium (Ti) substrate						
As-deposited	10	300	0.0025	41.20	20012	150
Annealed	12	315	0.0037	42.32	13333	250
Etched	16	315	0.0047	47.14	4871	333
Stainless Steel (S.S.) substrate						
As-deposited	5	63	0.0004	41.42	2732	25
Annealed	20	66	0.0011	41.66	1615	30
Etched	30	66	0.0020	50.50	714	40
FTO coated glass substrate						
As-deposited	800	209	0.154	46.05	68.75	4.40
Annealed	931	240	0.248	57.4	6.08	6.28
Etched	1006	251	0.298	59.5	3.80	7.33

It is seen that  $R_s$  and  $R_{sh}$  changes favorably on surface treatments. The process of annealing increases the packing density and strong adhesion to the substrates. Etching process contribute to the increase in the junction area so that

increase in RS is observed. For FTO coated glass substrate based PEC cells the remarkable improvement in efficiency is observed than that of metallic substrates based PEC cells. This can be attributed to the low  $R_s$  ( $\sim 3.88 \Omega$ ) and high  $R_{sh}$  ( $\sim 7.33 \text{ k}\Omega$ ) of FTO coated based PEC cells compared to metallic substrate based PEC cells. In spite of high  $R_{sh}$  for metallic substrate based PEC cells their  $R_s$  is large ( $\sim \text{K}\Omega$ ) which results in lower efficiency of PEC cells.

The photovoltage rise and decay curve reveals that the increase in photovoltage is almost instantaneous. The decay constant, calculated from the slope of  $\log V_{oc}$  versus of decay curve, is found to be 1.18.

The spectral response of the PEC cell with film on FTO glass is studied in the wavelength range of 400 to 800 nm. It is seen that the  $I_{sc}$  and quantum efficiency ( $Q_F$ ) attains the maximum at ( $\approx 675 \text{ nm}$ ) and decreases with further increase in  $\lambda$ . The lower  $Q_F$  on the higher energy side is due to the strong absorption of light in the polyiodide electrolyte and larger amount of surface recombination of the photogenerated minority carriers. The band gap energy, obtained by extrapolating the straight portion of  $(Q_F h\nu)^2$  versus  $h\nu$  plot to energy axis at  $\alpha=0$ , of  $\text{Sb}_2\text{S}_3$  is found to be 1.73 eV. The slope of plot  $(Q_F)^{-1}$  versus  $(\alpha)^{-1}$  gives the minority carrier diffusion length ( $L_p$ ) to be  $0.033 \mu\text{m}$ .

The plot of  $C^{-2}$  versus voltage is used to determine the flat band potential for  $\text{Sb}_2\text{S}_3$  based PEC cell. Positive slopes of the plots again confirms the  $n$ - type conductivity of  $\text{Sb}_2\text{S}_3$  thin films. The dispersion in Mott – Schottky plots is attributed to the rough surface topography of the thin films. From the

slopes  $C^{-2}$  versus  $V$  plots, the values of donor density ( $N_D$ ) are calculated. From the value of  $N_D$ , the density of states in conduction band ( $N_C$ ) is calculated. From these values, the amount of band bending ( $V_{bb}$ ), barrier height ( $V_B$ ) and locations of the band edges of  $Sb_2S_3$  have been determined. Based on these parameters, the width of depletion layer ( $W$ ) is calculated. Summary of results obtained from Mott – Schottky plots for  $Sb_2S_3$  film on various substrates is given in following table.

Sr. No.	Physical parameter	Value obtained on		
		Ti	S.S.	FTO
1.	Electrolyte used	$I^3/I^-$	$I^3/I^-$	$I^3/I^-$
2.	$E_{f,redox}$ (eV <sub>SCE</sub> )	0.307	0.307	0.307
3.	$V_{fb}$ (eV <sub>SCE</sub> )	(0.050	(0.115	(0.260
4.	Donor concentration, $N_D$ (cm <sup>-3</sup> )	$1.095 \times 10^{12}$	$4.81 \times 10^{10}$	$2.12 \times 10^{10}$
5.	Density of states in conduction band, $N_C$ , (cm <sup>-3</sup> )	$1.17 \times 10^{18}$	$1.17 \times 10^{18}$	$1.17 \times 10^{18}$
6.	$E$ ( $E_F$ (eV <sub>SCE</sub> ))	0.359	0.440	0.461
7.	Band bending $V_{bb}$ (eV <sub>SCE</sub> )	0.350	0.415	0.560
8.	Barrier height, $V_B$	0.709	0.855	1.0221
9.	Depletion width, $W$ ( $\mu$ m)	0.079	0.414	0.724
10.	Conduction band edge, $E_C$ (eV <sub>SCE</sub> )	(0.40	(0.58	(0.82
11.	Valence band edge, $E_V$ (eV <sub>SCE</sub> )	1.40	1.22	0.98
12.	Carrier type	$n$	$n$	$n$

The difference in observed location of the bands and the various

values for the films deposited on three different substrates is due to the difference in grain size and defect density; as the films were prepared at two different temperatures, of the films. As we go from Ti to FTO substrates,  $W$  goes on increasing which reflects the increase in grain size and concurrent decrease in the scattering by grain boundaries. Relatively less  $R_s$  and higher  $ff$  for the films prepared on FTO coated glass substrates also supports these results.

**Chapter – VIII** focuses on the use of  $Sb_2S_3$  thin films on metallic substrates as septum electrode in rechargeable redox storage cells.  $Sb_2S_3$  films are used as a separator of the two redox electrolytes in two compartments. The redox electrolyte in the first compartment was 0.5 M polyiodide While 1M polysulphide and 0.1 M ferri – ferrocyanide were the electrolytes in second compartments for S. S. and Ti substrates based semiconductor – septum storage cells. Thin film of  $Sb_2S_3$  of (2.2 cm X 2.2 cm) = 4.84 cm<sup>2</sup> area deposited on stainless substrate was inserted in a rectangular buy of glass (2.2 cm X 2.2 cm) to form two compartments. The photoelectrode compartment was filled with polyiodide and another electrolyte in second compartment was 1M polysulphide.

Another cell consists of two separate rectangular compartments (2.5 cm X 2.5 cm X 2.5 cm) of Bakelite with 1 cm<sup>2</sup> diameter holes drilled on their sides. The  $Sb_2S_3$  film deposited on titanium substrate was then fixed between two compartments, drilled walls being in contact with the film and

titanium respectively. 0.1 M ferri–ferrocyanide electrolyte was filled in another compartment. The cells were charged continuously for 2 hours. Photovoltage gets saturated in around 1 hour and then remains constant. The discharging of the cells is relatively faster during first 60 minutes, then it is quite slow. Thus the cell works not only as a generator but also the storage of electricity.

Semiconductor / liquid junction cells represents a rapidly advancing field (from 1 to 19 % efficiency). Both basic and practical questions remain to be resolved. The limiting efficiency for any one cell depends on the band gaps(s) of the semiconductors(s) used, but the nature of the electroactive materials in the liquid electrolyte solution can control the barrier height, and hence open–circuit photovoltage. Study of interface energetics could be undertaken with the objective of increasing the barrier height to value as close to the band gap as possible. It is possible that understanding and manipulation of interfacial charge transfer kinetics at semiconductor / liquid junction could led to a system having significant advantages over an all solid state photovoltaic cells.